Roles of MED1 in Quiescence of Hair Follicle Stem Cells and Maintenance of Normal Hair Cycling

Takeshi Nakajima[1], Shigeki Inui[1], Tomohiro Fushimi[1], Fumihito Noguchi[1], Yutaka Kitagawa[1], Janardan K. Reddy[2] and Satoshi Itami[1]

MED1 (mediator complex subunit 1) is expressed by human epidermal keratinocytes and functions as a coactivator of several transcription factors. To elucidate the role of MED1 in keratinocytes, we established keratinocyte-specific *Med1*-null (*Med1*$^{epi-/-}$) mice using the *K5Cre/LoxP* system. Development of the epidermis and appendages of *Med1*$^{epi-/-}$ mice were macroscopically and microscopically normal until the second catagen of the hair cycle. However, the hair cycle of *Med1*$^{epi-/-}$ mice was spontaneously repeated after the second telogen, which does not occur in wild-type (WT) mice. Hair follicles of *Med1*$^{epi-/-}$ mice could not enter anagen after 6 months of age, resulting in sparse pelage hair in older *Med1*$^{epi-/-}$ mice. Interfollicular epidermis (IFE) of *Med1*$^{epi-/-}$ mice was acanthotic and more proliferative than that of WT mice, whereas these findings were less evident in older *Med1*$^{epi-/-}$ mice. Flow cytometric analysis revealed that the numbers of hair follicle bulge stem cells were reduced in *Med1*$^{epi-/-}$ mice from a few months after birth. These results suggest that MED1 has roles in maintaining quiescence of keratinocytes and preventing depletion of the follicular stem cells.

Journal of Investigative Dermatology (2013) **133,** 354–360; doi:10.1038/jid.2012.293; published online 30 August 2012

INTRODUCTION

MED1 (also named PBP/TRAP220) has been shown to interact with several nuclear receptors, including thyroid hormone receptor, vitamin D receptor (VDR), peroxisome proliferator–activated receptor (PPAR), retinoic acid receptor, and retinoid X receptor (RXR) (Zhu *et al.*, 1997; Ge *et al.*, 2002). MED1 is also known to interact with the transcription factors p53, BRCA1 (breast cancer 1, early onset), and GATA binding protein (Frade *et al.*, 2000; Crawford *et al.*, 2002; Wada *et al.*, 2004; Stumpf *et al.*, 2006, 2010). Therefore, MED1 influences a wide range of transcription signaling pathways, and disruption of MED1 can cause the malfunction of several transcription factors. *Med1*-null mice are lethal by embryonic day 11.5 because of impaired placenta function (Zhu *et al.*, 2000; Landles *et al.*, 2003) and defects in the heart, liver, central nervous system, and eyes (Ito *et al.*, 2000; Crawford *et al.*, 2002). Because embryonic fibroblasts derived from *Med1* knockout mice reportedly show decreased thyroid hormone receptor function, but not retinoic acid receptor/RXR- or p53-dependent transactivation (Ito *et al.*, 2000), MED1 functions in specific intracellular signaling pathways that depend on the cell type. Although increasing evidence suggests that MED1 has various roles in regulating the differentiation and proliferation of keratinocytes, its precise function in keratinocytes has not been fully elucidated. To investigate the function(s) of MED1 in keratinocytes *in vivo*, we generated and analyzed keratinocyte-specific *Med1*-disrupted mice.

RESULTS

Absence of MED1 protein in keratinocytes derived from *Med1*$^{epi-/-}$ mice

To generate *K5Cre+;Med1*$^{flox/flox}$ (*Med1*$^{epi-/-}$) mice, *Med1*$^{flox/flox}$ mice, in which *loxP* sites were introduced into the *Med1* gene (Jia *et al.*, 2004), were first crossed with *K5Cre* mice, in which the Cre recombinase gene had been inserted downstream of the human keratin 5 (K5) promoter (Tarutani *et al.*, 1997), after which the F1 *K5Cre+;Med1*$^{flox/+}$ mice were crossed with *Med1*$^{flox/flox}$ mice. To confirm the disruption of MED1 protein in *Med1*$^{epi-/-}$ keratinocytes, we performed immunoblotting using protein extracts of keratinocytes derived from control *K5Cre-;Med1*$^{flox/flox}$ (wild type (WT)) and from *Med1*$^{epi-/-}$ mice. As shown in Figure 1a, the 205 kDa protein band (arrow) corresponding to MED1 was detected only in WT keratinocytes. Immunohistochemically, in contrast to the MED1 expression in the interfollicular epidermis (IFE; Figure 1b) and in the follicular

[1]*Department of Regenerative Dermatology, Graduate School of Medicine, Osaka University, Suita, Osaka, Japan and* [2]*Department of Pathology, Feinberg School of Medicine, Northwestern University, Chicago, Illinois, USA*

Correspondence: Takeshi Nakajima, Department of Regenerative Dermatology, Graduate School of Medicine, Osaka University, 2-2 Yamadaoka, Suita, Osaka 565-0871, Japan.
E-mail: nakajima@r-derma.med.osaka-u.ac.jp

Abbreviations: BRCA1, breast cancer 1, early onset; IFE, interfollicular epidermis; K5, keratin 5; MED1, mediator complex subunit 1; PPAR, peroxisome proliferator–activated receptor; RXR, retinoid X receptor; SOX9, SRY (sex-determining region Y)-box 9; VDR, vitamin D receptor; WT, wild type

Received 31 October 2011; revised 16 July 2012; accepted 19 July 2012; published online 30 August 2012

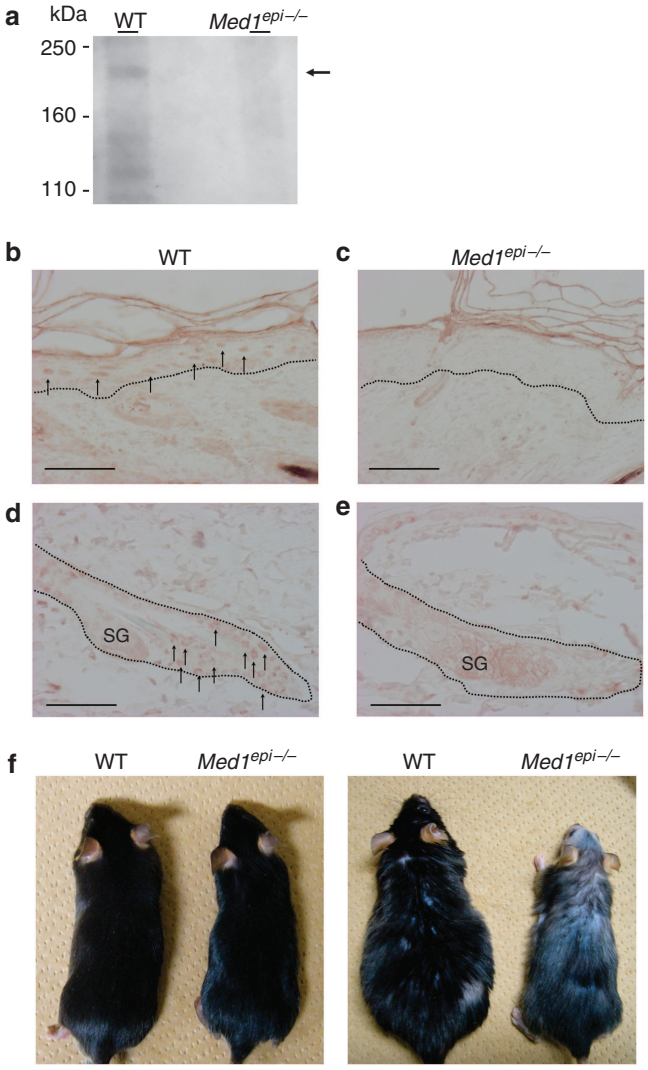

Figure 1. MED1 (mediator complex subunit 1) protein is absent in keratinocytes derived from *Med1*$^{epi-/-}$ mice. (**a**) Immunoblotting confirms the deletion of MED1 protein (arrow) in *Med1*$^{epi-/-}$ keratinocytes. (**b**–**e**) Immunohistochemical staining of MED1 in the skin from wild-type (WT) mice and *Med1*$^{epi-/-}$ mice. Bar = 50 μm. Nuclear staining of MED1 in the (**b**) epidermis and in the (**d**) bulge is not detected in *Med1*$^{epi-/-}$ skin (**c**, **e**). Broken lines define the border between the dermis and epidermis. Arrows denote low but real nuclear staining of MED1 in interfollicular epidermis (IFE) and follicular bulge keratinocytes. SG, sebaceous gland. (**f**) The stature of *Med1*$^{epi-/-}$ mice is smaller 10 weeks after birth (left panel). The difference is more significant 1 year after birth (right panel). The pelage hair of aged *Med1*$^{epi-/-}$ mice is sparse compared with that of WT mice.

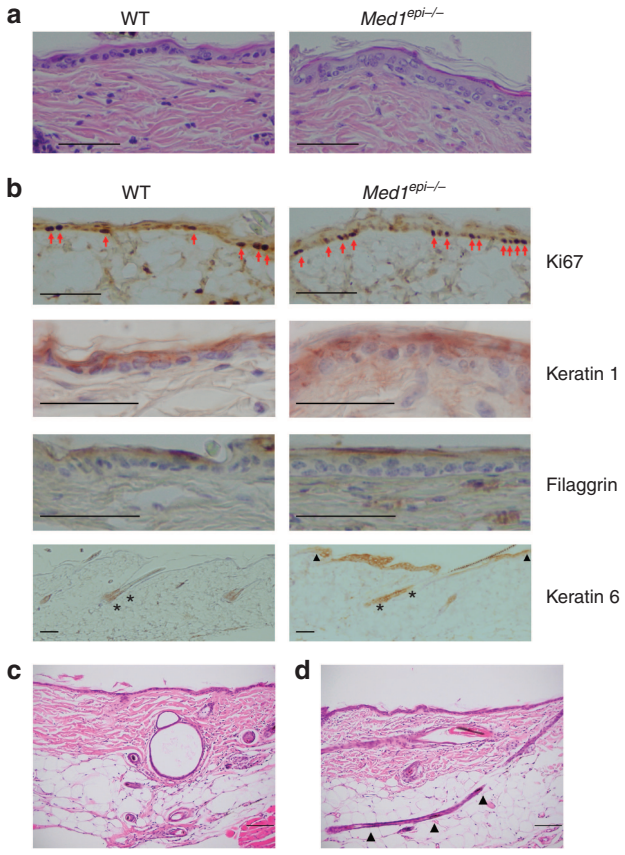

Figure 2. Histological analysis of *Med1*$^{epi-/-}$ skin. (**a**) In contrast to the 2–3 cell–layered epidermis in 2-month-old wild-type (WT) mice, the epidermis of *Med1*$^{epi-/-}$ mice consists of 2–5 cell layers. Bar = 50 μm. (**b**) Ki67-positive keratinocytes are more frequently detected in *Med1*$^{epi-/-}$ interfollicular epidermis (IFE; arrows). The expression patterns of keratin 1 and filaggrin in 2-month-old IFE were not perturbed in the *Med1*$^{epi-/-}$ skin. Although keratin 6 (K6) is not expressed in the IFE of WT mice, it is focally expressed in the *MED1*$^{epi-/-}$ IFE (both ends are indicated by triangles). A broader area in *Med1*$^{epi-/-}$ telogen hair follicles is positive for K6 (asterisks). Bar = 50 μm. (**c**) Large dermal cysts and (**d**) anagen-like thin hair follicles are observed in an 11-month-old and a 5-month-old *Med1*$^{epi-/-}$ mouse, respectively (arrows indicate hair shafts). Bar = 100 μm.

bulge (Figure 1d) of WT mice, MED1 was not detected in any of those locations in *Med1*$^{epi-/-}$ mice (Figure 1c and e).

Skin and skin appendages develop normally at birth, but body growth retardation and sparse hair gradually become apparent in *Med1*$^{epi-/-}$ mice

The body weight and body length of *Med1*$^{epi-/-}$ mice were comparable to those of their WT siblings at birth. However, the growth retardation of *Med1*$^{epi-/-}$ mice became significant from 3 weeks of age and later, although the cause of the growth retardation has not been elucidated (Figure 1f and Supplementary Figure S1 online). The development of *Med1*$^{epi-/-}$ skin was normal at birth, and both WT and *Med1*$^{epi-/-}$ mice were covered with normal hair within several days macroscopically. However, the pelage hair of *Med1*$^{epi-/-}$ mice became sparse from ~6 months after birth, and, in most cases, vibrissae were lost (Figure 1f).

Proliferation and differentiation of the IFE and skin appendages in *Med1*$^{epi-/-}$ mice

Microscopically, the IFE, the horny layer, and the skin appendages were formed normally in newborn *Med1*$^{epi-/-}$ mice (Supplementary Figure S2a online). Their epidermis became significantly thicker than that of WT mice when they were 2 months of age; however, the difference became less significant when they were more than 1 year old (Figure 2a, Table 1 and Supplementary Figure S2 online). The granular and horny layers were normally formed in the skin of *Med1*$^{epi-/-}$ mice during this observation period. To clarify

Table 1. Relative epidermal thickness of *Med1*$^{epi-/-}$ mice

	3 Days old	3 Weeks old	2 Months old	6 Months old	>1 Year old
Relative epidermal thickness of *Med1*$^{epi-/-}$	0.98	1.03	1.17*	1.20	0.92

Relative epidermal thickness of *Med1*$^{epi-/-}$ mice compared with wild-type (WT) mice at the indicated time points. The difference in epidermal thickness between these mice was statistically significant at 2 months of age. The thicker epidermis in *Med1*$^{epi-/-}$ mice became less apparent ~1 year after birth. Student's *t*-test was used for statistical analysis.
*$P<0.05$.

the mechanism of the hyperplastic epidermis in *Med1*$^{epi-/-}$ mice, differentiation and proliferation markers of keratinocytes were characterized using immunohistochemical analysis. Ki67-positive proliferating keratinocytes in 2-month-old *Med1*$^{epi-/-}$ mice were 1.57 times more frequently observed compared with their WT counterparts ($n=3$, $P<0.05$); however, no remarkable difference was observed in staining patterns for K1 and filaggrin (Figure 2b), nor for K5 (data not shown). K6 is expressed in the companion layer of normal hair follicles and in the IFE during wound healing, but not in normal IFE (Moll *et al.*, 2008) in WT mice. However, K6 was expressed focally in the IFE and in broader parts of telogen hair follicles of *Med1*$^{epi-/-}$ mice (Figure 2b). This result also suggests that keratinocytes in the IFE of *Med1*$^{epi-/-}$ mice are more proliferative. These staining results indicate that the abnormal thickness of the epidermis in *Med1*$^{epi-/-}$ mice can be attributed to increased proliferation rather than to impaired differentiation. In contrast to the thick epidermis, the dermis of *Med1*$^{epi-/-}$ mice is thinner than that of WT mice (Supplementary Figure S3 online), although *Med1*$^{epi-/-}$ dermal fibroblasts are supposed to express MED1 at the same level as the WT counterparts. It is thus reasonable to speculate that cytokines secreted from keratinocytes of *Med1*$^{epi-/-}$ mice inhibit the proliferation of fibroblasts and/or the production of matrix proteins in the dermis, whereas key soluble factors that influence the thickness of the dermis in *Med1*$^{epi-/-}$ mice are unknown. Other microscopic abnormalities in *Med1*$^{epi-/-}$ mouse skin include hypertropic sebaceous glands, cyst formation, and abnormally thin anagen-like hair follicles (Figure 2c and d, and Supplementary Figure S3 online). These anagen-like follicles exist in the pink skin where most hair follicles are in the telogen stage of the hair cycle, and grow as deep as normal anagen hair follicles; however, the epithelial sheaths of these follicles are thinner. All these abnormal features were apparent from several months after birth.

The growth phase of the hair cycle is frequently induced in *Med1*$^{epi-/-}$ mice, but the total number of hair cycles over the lifetime is limited

Although young *Med1*$^{epi-/-}$ mice produced normal hair, their hair became progressively sparse after ~6 months of age (Figure 1f). Therefore, we examined the pattern of the hair cycle in *Med1*$^{epi-/-}$ mice. The stages of the hair cycle were determined by the color of the skin in C57BL/6 mice. It is assumed that hair follicles in black skin are in anagen (growing phase), those in gray skin are in catagen (regressing phase), and those in pink skin are in telogen (resting phase) (Müller-Röver *et al.*, 2001). There was no obvious difference between *Med1*$^{epi-/-}$ and WT mice in the first and second hair cycles, which start soon after birth and ~22 days after birth, respectively. As the third anagen in WT mice starts sporadically in small areas of the skin to form mosaic patterns, the second telogen period ranges from 12 to 40 days depending on the body site (Plikus *et al.*, 2008). Therefore, the dorsal skin of WT mice over 7 weeks of age is mostly in telogen as shown in the upper panels of Figure 3a. In contrast to the long telogen in WT mice, hair follicles of *Med1*$^{epi-/-}$ mice entered the third anagen stage synchronously over the entire dorsal skin ~7 days after the second telogen without any anagen-inducing stimuli. In addition, *Med1*$^{epi-/-}$ mice had a highly simplified hair cycle–domain pattern that forms bands of black skin (Figure 3a). To further investigate the hair cycles of *Med1*$^{epi-/-}$ mice, pelage hair on the dorsal skin of 8-week-old *Med1*$^{epi-/-}$ mice was depilated only once and their skin color was recorded. To observe the color of the skin after depilation, the hair was trimmed by clippers so that mechanical stimuli do not induce anagen thereafter. Synchronized depilation-induced anagen was observed in both WT and Med1$^{epi-/-}$ mice, followed by spontaneous catagen and telogen. We microscopically confirmed that both WT and *Med1*$^{epi-/-}$ hair follicles were in anagen 15 days after depilation, and these hair follicles similarly expressed K31 at this time point (data not shown). Although synchronized anagen was no longer observed in WT mice thereafter, spontaneous induction of anagen over the whole dorsal skin was repeated three additional times in *Med1*$^{epi-/-}$ mice (Figure 3b). At ~100 days after depilation, most of the hair follicles of the *Med1*$^{epi-/-}$ dorsal skin stayed in telogen and the mice produced only sparse hair. This finding is consistent with the observation that most hair follicles of *Med1*$^{epi-/-}$ mice were in telogen after ~6 months of age. From these results, we conclude that hair follicles in *Med1*$^{epi-/-}$ mice are able to repeat synchronized hair cycles until ~6 months of age; however, most hair follicles stop generating hair after 6 months of age.

Analysis of the pelage hair shafts of *Med1*$^{epi-/-}$ mice

Pelage hairs of mice are classified into four subtypes (Sundberg and Hogan, 1994). By microscopic observation, we confirmed that there were all four hair subtypes on *MED1*$^{epi-/-}$ mice. The average diameter of 7-week-old *Med1*$^{epi-/-}$ guard hairs was $38.5\pm3.6\,\mu m$ (mean ± SD), whereas that of WT was $48.1\pm5.9\,\mu m$; the difference is statistically significant by Student's *t*-test ($n=4$, $P<0.001$). The average diameter of *Med1*$^{epi-/-}$ zigzag hair was $16.8\pm2.0\,\mu m$, which was also significantly smaller than that of WT, $19.9\pm3.0\,\mu m$ ($n=4$, $P<0.001$). A significant difference in hair shaft diameter was similarly observed in mice aged between 6 and 8 months (data not shown). In

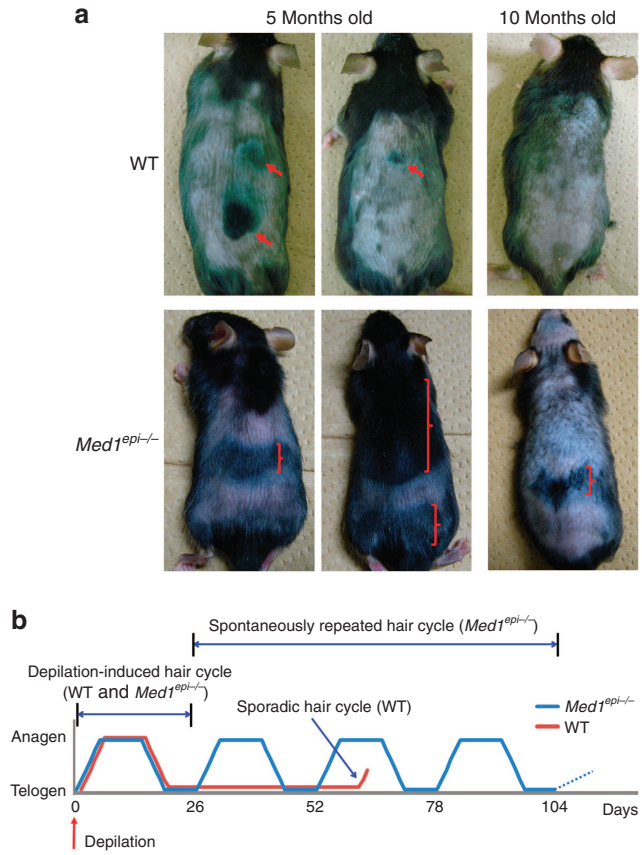

Figure 3. Hair cycle and hair cycle–domain pattern of *Med1*$^{epi-/-}$ mice. (**a**) The wild-type (WT) and *Med1*$^{epi-/-}$ dorsal pelage hair was trimmed at indicated age points. The upper panels demonstrate small dotted areas of anagen in WT skin (arrows). Without any anagen-inducing stimuli, broader areas of the *Med1*$^{epi-/-}$ skin are in anagen, demonstrating black skin bands while repeating extraordinary hair cycles (brackets). (**b**) Dorsal pelage hairs of 8-week-old *Med1*$^{epi-/-}$ mice and WT mice were depilated by hand. Synchronized depilation-induced anagen was observed in both WT and *Med1*$^{epi-/-}$ skin. Following the depilation-induced hair cycle, spontaneous induction of synchronized anagen over the entire dorsal skin was repeated consecutively three additional times only in *Med1*$^{epi-/-}$ mice. Three *Med1*$^{epi-/-}$ mice were used for the analysis and representative results are shown.

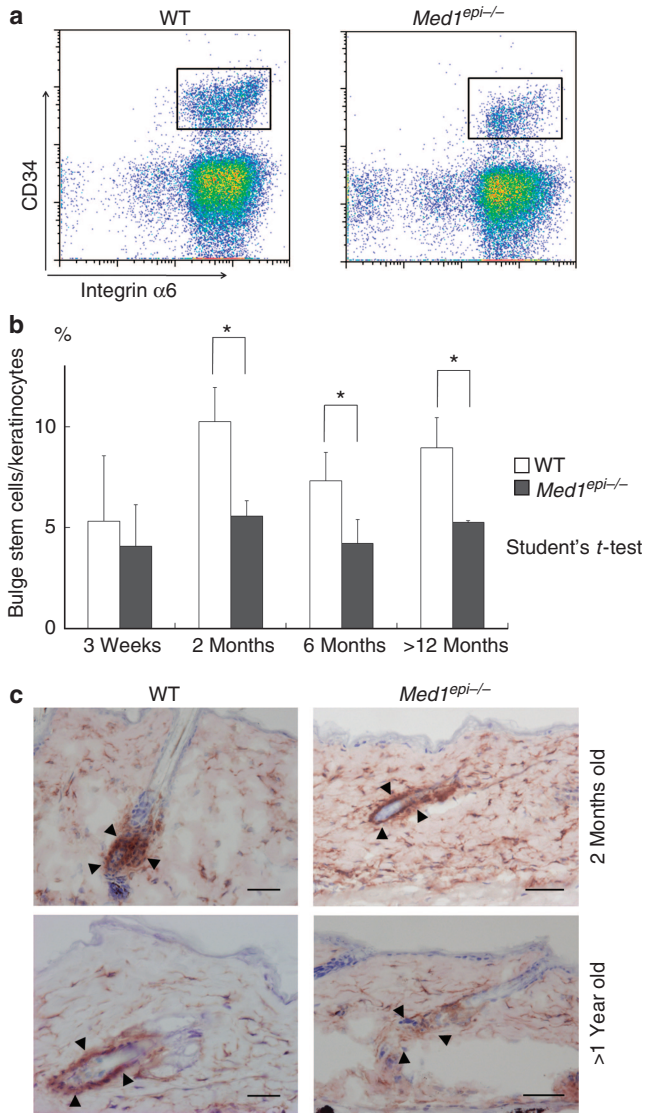

Figure 4. Hair follicle bulge stem cells are decreased in adult *Med1*$^{epi-/-}$ mice. (**a**) Keratinocytes were isolated from wild-type (WT) and *Med1*$^{epi-/-}$ littermates at the indicated ages and analyzed by flow cytometry. Representative cell-sorting profiles from 2-month-old WT and *Med1*$^{epi-/-}$ keratinocytes are shown. (**b**) Ratio of follicular stem cells. Keratinocytes were derived from WT and *Med1*$^{epi-/-}$ littermates at 3 weeks, 2 months, 6 months, and >12 months of age ($n=3$). Student's *t*-test was used for determining statistical significance between the ratios. *$P \leqslant 0.05$. (**c**) Immunohistochemical staining shows CD34-positive cells in 2-month-old and 18-month-old WT hair follicles and in 2-month-old and 13-month-old *Med1*$^{epi-/-}$ hair follicles. Arrowheads indicate the hair bulge areas, in which CD34 is positively stained. Bar = 50 μm.

addition, auchene and zigzag hairs of *Med1*$^{epi-/-}$ mice tended to have a decreased bending angle compared with WT littermates (Supplementary Figure S4a online). In the bending part of the auchene and the zigzag hairs, the distance between the bands of pigmentation was shorter in hair from *Med1*$^{epi-/-}$ mice (Supplementary Figure S4b online); however, the physiological role of the pigmentation in the hair has not been elucidated.

Hair bulge stem cells are depleted in adult *Med1*$^{epi-/-}$ mice

Although the IFE was acanthotic as a result of the hyperproliferation of keratinocytes and the hair cycles were repeated more frequently in *Med1*$^{epi-/-}$ mice, these features were lost when the mice were 6 months to 1 year old. To evaluate the numbers of bulge stem cells in *Med1*$^{epi-/-}$ mice, we quantified bulge stem cells by FACS using a combination of antibodies against the cell surface proteins CD34 and integrin α6 (Trempus *et al.*, 2003). Bulge stem cells form the CD34-positive and integrin α6–positive population (Figure 4a). The percentage of these stem cells to the total live epithelial cells during the telogen stage of the hair cycle was calculated. As a result, no statistically significant difference was detected between WT and *Med1*$^{epi-/-}$ mice 3 weeks after birth. However, the percentage of stem cells in the skin of *Med1*$^{epi-/-}$ mice was significantly lower at 2 months after birth and thereafter (Figure 4b). In contrast to the

FACS results, the reduction of CD34-positive bulge cells in 2-month-old *Med1*$^{epi-/-}$ mice was less apparent immunohistochemically (Figure 4c). However, the bulge areas of *Med1*$^{epi-/-}$ hair follicles in mice aged ⩾1 year were obviously weakly stained by CD34 as compared with those of aged WT hair follicles (Figure 4c). Immunohistochemical staining using another hair follicle bulge marker, K15, also indicated that bulge cells decreased with aging only in *Med1*$^{epi-/-}$ hair follicles (Supplementary Figure S5 online).

Expression of *Sox9* is reduced in *Med1*$^{epi-/-}$-cultured keratinocytes

To elucidate the mechanism(s) underlying the loss of quiescence in bulge stem cells of *Med1*$^{epi-/-}$ mice, we compared the gene expression patterns of *Med1*$^{epi-/-}$-derived keratinocytes with their WT counterparts by microarray analysis. Several genes related to stem cell maintenance and the cell cycle, including *Sox9*, *Runx1*, *Trp63*, and *Cyclin G2*, were detected (Supplementary Table S1 online). Although the downregulation of *Sox9* was confirmed, the change in *Runx1* expression was not detected by semi-quantitative reverse transcription PCR (data not shown). SOX9 (SRY (sex-determining region Y)-box 9) is expressed in the upper outer root sheath cells including the bulge, and is functionally most related to bulge stem cell maintenance and hair cycle regulation. Previous reports demonstrated that SOX9 is essential for the maintenance of bulge stem cells (Vidal *et al.*, 2005; Nowak *et al.*, 2008). Indeed, we clearly detected the reduced expression of SOX9 in *Med1*$^{epi-/-}$-cultured keratinocytes by immunoblotting as well (Figure 5), suggesting regulation of SOX9 expression by MED1. Although we could not detect significant reduction in *Sox9* expression in *in vivo Med1*$^{epi-/-}$ skin of 6-month-old mice, neither by quantitative real-time PCR nor by immunoblotting (data not shown), reduced expression of SOX9 in the bulge cells of some *Med1*$^{epi-/-}$ hair follicles was observed by immunohistochemistry (Supplementary Figure S6 online).

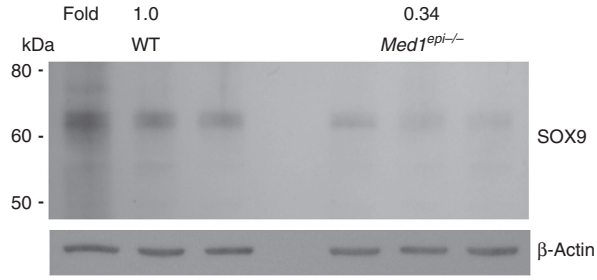

Figure 5. Reduced expression of SOX9 (SRY (sex-determining region Y)-box 9) in *Med1*$^{epi-/-}$ keratinocytes. Cultured keratinocytes were derived from wild-type (WT) and *Med1*$^{epi-/-}$ newborn skin as described in the Materials and Methods. Immunoblot analysis demonstrates that the expression of SOX9 in *Med1*$^{epi-/-}$-cultured keratinocytes is lower than that in the WT counterparts. Quantification of band intensity was performed by ImageJ, version 1.44 software (developed at the National Institutes of Health), and the average intensity of *Med1*$^{epi-/-}$ keratinocytes is expressed in terms of fold increase in WT.

DISCUSSION

We established keratinocyte-specific *Med1*-null mice and found several phenotypes that resemble some nuclear receptor–null mice. The IFE of *Vdr*-null (*VdrKO*) mice and of keratinocyte-specific *Rxrα*-null (*Rxrα*$^{epi-/-}$) mice is hyperplastic compared with that of their WT counterparts (Li *et al.*, 2001; Bikle *et al.*, 2006). Ablation of *Vdr* is associated with a gradual decrease in keratinocyte stem cells (Cianferotti *et al.*, 2007). Keratinocytes of *Pparβ*-null (*PparβKO*) mice are also more proliferative than those of WT mice (Peters *et al.*, 2000). As shown in our study, the epidermis of *Med1*$^{epi-/-}$ mice is hyperproliferative, and follicular stem cells of *Med1*$^{epi-/-}$ mice decrease with age. These phenotypes in *Med1*$^{epi-/-}$ mice are possibly related to the function of MED1 as a coactivator of VDR and PPARβ in keratinocytes. However, the characteristic hair structure and hair cycle in *Med1*$^{epi-/-}$ mice are different from those of *VdrKO*, *Rxrα*$^{epi-/-}$, and *PparβKO* mice.

Among other genetically modified mice, *K14-Noggin* mice share characteristic phenotypes with *Med1*$^{epi-/-}$ mice with regard to the hair cycle, hair cycle domains, enlargement of the sebaceous gland, thickness of the epidermis, and increased numbers of Ki-67-positive cells in the epidermis (Plikus *et al.*, 2004, 2008; Sharov *et al.*, 2009). Furthermore, *K14-Noggin* mice also showed no abnormality in epidermal differentiation, which was evidenced by their expression of loricrin (Sharov *et al.*, 2009). However, no evidence has been obtained regarding the involvement of the Mediator complex in BMP/Smad1/5/8 signaling. We could not detect a direct interaction between MED1 and Smad1/5/8 (data not shown). The repeated synchronized anagen entry on the dorsal skin has also been reported in *fuzzy* mice (Mecklenburg *et al.*, 2005), in which the *Sgk3* gene is mutated (Campagna *et al.*, 2008), and in *Msx2*-null mice (Ma *et al.*, 2003). However, the hair cycles of these mice were different from those of *Med1*$^{epi-/-}$ mice in that the telogen period was longer in *Msx2*-null mice and the anagen follicles of *fuzzy* mice regressed earlier. In other studies, the follicles of *Lhx2KO* mice precociously entered the next hair cycle with a shorter period of telogen, and they exhibited diminished expression of CD34, indicating its essential role in the quiescence of hair follicle stem cells (Rhee *et al.*, 2006). Although those phenotypical similarities suggested the possibility that MED1 is involved in these signals in keratinocytes, no evidence for such an involvement has been obtained. While we were revising this paper, another group reported keratinocyte-specific *Med1*-null mice (Oda *et al.*, 2012). Their results also indicated hyperproliferative IFE and abnormality of hair cycle by the absence of MED1. Our results demonstrated these abnormalities in detail, and revealed depletion of bulge stem cells in *Med1*$^{epi-/-}$ hair follicles as well.

In WT mice, CD34+ and integrin α6+ follicular stem cells were detected similarly in both young and old mice by FACS analysis and by whole-mount immunohistochemistry (Giangreco *et al.*, 2008). The expression of hair follicle stem cell markers was also preserved in aged human follicular bulge areas (Rittie *et al.*, 2009). These observations indicate that follicular stem cells are not depleted in normal conditions until the end of life in humans and mice. On the contrary, it was reported that, by repeated plucking of mouse

vibrissae, half of the follicles stopped producing whiskers before 10 successive pluckings and then formed cysts near the dermal papillae (Ibrahim and Wright, 1978). This result suggests that the follicular stem cells might be exhausted when hair cycles are repeated too frequently. It is possible to speculate that the follicular stem cells of *Med1*$^{epi-/-}$ mice were depleted by the frequent hair cycles. However, our FACS results indicated that the number of CD34-positive bulge stem cells in *Med1*$^{epi-/-}$ mice is reduced as early as 2 months of age, suggesting that the reduction in CD34-positive bulge stem cells is not merely attributable to depletion by repeated hair cycles.

SOX9 has been reported to be involved in the maintenance of bulge stem cells (Vidal *et al.*, 2005). As it has been reported that SOX9 interacts with the Mediator complex (Zhou *et al.*, 2002), disruption of MED1 can possibly lead to reduced transactivation of SOX9 in keratinocytes. In addition, our results demonstrated that expression of SOX9 is regulated by MED1 in keratinocytes, although a definite result was obtained only by using cultured keratinocytes. These reports suggested the possibility that the disruption of MED1 might activate bulge stem cells by reducing the transactivation of SOX9, resulting in the eventual depletion of stem cells.

Our microarray results suggest that MED1 in keratinocytes regulates dermal thickness, possibly through secretory proteins. Although secretory proteins, including transforming growth factor-β, are known to increase dermal thickness, it has yet to be elucidated how dermal thickness is reduced by secretory protein(s). Some of the secretory proteins regulated by MED1, including follistatin, matrix metalloproteinase-3, and platelet-derived growth factor, need to be investigated for the regulation of dermal thickness by keratinocytes in *Med1*$^{epi-/-}$ mice, because follistatin is a potential inhibitor of transforming growth factor-β signaling, matrix metalloproteinases can degrade extracellular matrix, and platelet-derived growth factor is a profibrotic factor (Jinnin, 2010).

The roles of MED1 in keratinocytes included the regulation of quiescence of hair follicle stem cells and maintenance of normal hair shaft formation and hair cycling, as well as regulation of dermal thickness. Although the precise mechanisms of how MED1 regulates these various roles in the skin have yet to be elucidated, our study suggested that MED1 might be related at least in part to the functions of several transcription factors, including VDR, PPARβ, and SOX9, in keratinocytes. As MED1 has such roles in the skin, MED1 can be one of the target molecules for treatments of several skin disorders, including chronic skin ulcer, alopecia, and scleroderma.

MATERIALS AND METHODS

Generation of the *Med1*-conditional null mutation in epidermal keratinocytes

Med1$^{flox/flox}$ mice (Jia *et al.*, 2004) were mated with *K5Cre* mice (Tarutani *et al.*, 1997) to generate F1 *K5Cre*+;*Med1*$^{flox/+}$ mice. The *K5Cre*+;*Med1*$^{flox/+}$ mice were then mated with *Med1*$^{flox/flox}$ mice to generate *K5Cre*+;*Med1*$^{flox/flox}$ mice (*Med1*$^{epi-/-}$). All mice were of C57BL/6 background. The mice were screened for the presence of the transgene by PCR using specific primers for the floxed *Med1* gene and the human *K5* gene according to previous reports (Tarutani *et al.*, 1997; Jia *et al.*, 2004). All animal studies were conducted according to the protocols approved by the Institutional Animal Care and Use Committee at Osaka University.

Keratinocyte isolation and culture

Skin of newborn mice was excised after the mice were killed with excessive anesthesia and were treated with dispase, followed by trypsin, to separate the epidermis from the dermis. Keratinocytes were seeded on type I collagen-coated dishes and were cultured in CnT07-conditioned culture medium (CELLnTEC, Bern, Switzerland). Keratinocytes were used for each experiment as a primary culture or after one passage.

Histological analysis of the skin

Skin specimens were fixed in 10% formalin and processed for embedding in paraffin, or were embedded in optimal cutting temperature compound (Tissue-Tek, Sakara Finetek, Tokyo, Japan) and snap-frozen in liquid nitrogen. Paraffin-embedded specimens were sectioned and stained with hematoxylin and eosin or were processed for immunohistochemical staining. For immunohistochemical staining, anti-filaggrin (M-290; 1:100; Santa Cruz Biotechnology, Santa Cruz, CA), anti-TRAP220 (C-19; 1:200; Santa Cruz Biotechnology), anti-Ki67 antigen (polyclonal; 1:500; Leica Microsystems, Newcastle Upon Tyne, UK), anti-mouse K1 (AF109; 1:100; Covance, Emeryville, CA), anti-mouse K6 (1:500; Covance), and anti-CD34 (RAM34; 1:50; BD Biosciences, San Jose, CA) antibodies were used. Technical details for immunohistochemical staining are described in the Supplementary Material online.

Immunoblot analyses

For immunoblot analysis, cultured keratinocytes were lysed in 2 × sample buffer (Invitrogen, Carlsbad, CA) supplemented with 5% 2-mercaptoethanol. Total protein extracts were subjected to 4–2% SDS-PAGE (Invitrogen) under reducing conditions, transferred to nitrocellulose membranes, and immunoblotted using anti-TRAP220 (C-19) antibody (1:2,000; Santa Cruz Biotechnology) or anti-SOX9 (H-90) antibody (1:2,000; Santa Cruz Biotechnology) and horseradish peroxidase–conjugated donkey anti-goat secondary antibody (1:10,000; Santa Cruz Biotechnology) or horseradish peroxidase–conjugated donkey anti-rabbit secondary antibody (1:15,000; GE Healthcare, Buckinghamshire, UK). The blots were visualized with ECL Plus Western blotting detection reagent (GE Healthcare).

Flow cytometry

The procedure used for flow cytometric analysis has been described previously (Nowak and Fuchs, 2009). Briefly, primary mouse keratinocytes were isolated from the dorsal skin of mice. Cells were labeled with phycoerythrin-conjugated anti-CD49f (clone GoH3) antibody (BD Biosciences), biotin-conjugated anti-CD34 (clone RAM34) antibody (eBioscience, San Diego, CA), and streptavidin–allophycocyanin conjugate (BD Biosciences). Cells were then analyzed using a FACScalibur (BD Biosciences) sorter and FlowJo analysis software (Tree Star, Ashland, OR).

Microarray analysis

Total RNAs were extracted from cultured keratinocytes derived from WT and from *Med1*$^{epi-/-}$ skin, and then biotinylated cRNA was

prepared and hybridized to Mouse Genome 430 2.0 arrays (Affymetrix, Santa Clara, CA). Detailed protocols have been described in the Supplementary Material online. The array results have been deposited in the Gene Expression Omnibus repository (http://www.ncbi.nlm.nih.gov/geo) under accession number GSE35406.

CONFLICT OF INTEREST

The authors state no conflict of interest.

ACKNOWLEDGMENTS

We thank Naoko Yamada, Saiko Ishii, and Ayako Sato for technical assistance. This work was supported in part by grants-in-aid from the Ministry of Education, Science, Sports and Culture of Japan (19790784, 21791075, and 23591644) and by a Japanese Dermatological Association basic medical research grant (Shiseido donation) to TN.

SUPPLEMENTARY MATERIAL

Supplementary material is linked to the online version of the paper at http://www.nature.com/jid

REFERENCES

Bikle DD, Elalieh H, Chang S *et al.* (2006) Development and progression of alopecia in the vitamin D receptor null mouse. *J Cell Physiol* 207:340–53

Campagna DR, Custodio AO, Antiochos BB *et al.* (2008) Mutations in the serum/glucocorticoid regulated kinase 3 (Sgk3) are responsible for the mouse fuzzy (fz) hair phenotype. *J Invest Dermatol* 128:730–2

Cianferotti L, Cox M, Skorija K *et al.* (2007) Vitamin D receptor is essential for normal keratinocyte stem cell function. *Proc Natl Acad Sci USA* 104:9428–33

Crawford SE, Qi C, Misra P *et al.* (2002) Defects of the heart, eye, and megakaryocytes in peroxisome proliferator activator receptor-binding protein (PBP) null embryos implicate GATA family of transcription factors. *J Biol Chem* 277:3585–92

Frade R, Balbo M, Barel M (2000) RB18A, whose gene is localized on chromosome 17q12-q21.1, regulates in vivo p53 transactivating activity. *Cancer Res* 60:6585–9

Ge K, Guermah M, Yuan CX *et al.* (2002) Transcription coactivator TRAP220 is required for PPAR gamma 2-stimulated adipogenesis. *Nature* 417:563–7

Giangreco A, Qin M, Pintar JE *et al.* (2008) Epidermal stem cells are retained in vivo throughout skin aging. *Aging Cell* 7:250–9

Ibrahim L, Wright EA (1978) The long term effect of repeated pluckings on the function of the mouse vibrissal follicles. *Br J Dermatol* 99:371–6

Ito M, Yuan CX, Okano HJ *et al.* (2000) Involvement of the TRAP220 component of the TRAP/SMCC coactivator complex in embryonic development and thyroid hormone action. *Mol Cell* 5:683–93

Jia Y, Qi C, Kashireddi P *et al.* (2004) Transcription coactivator PBP, the peroxisome proliferator-activated receptor (PPAR)-binding protein, is required for PPARalpha-regulated gene expression in liver. *J Biol Chem* 279:24427–34

Jinnin M (2010) Mechanisms of skin fibrosis in systemic sclerosis. *J Dermatol* 37:11–25

Landles C, Chalk S, Steel JH *et al.* (2003) The thyroid hormone receptor-associated protein TRAP220 is required at distinct embryonic stages in placental, cardiac, and hepatic development. *Mol Endocrinol* 17: 2418–35

Li M, Chiba H, Warot X *et al.* (2001) RXR-alpha ablation in skin keratinocytes results in alopecia and epidermal alterations. *Development* 128:675–88

Ma L, Liu J, Wu T *et al.* (2003) Cyclic alopecia' in Msx2 mutants: defects in hair cycling and hair shaft differentiation. *Development* 130:379–89

Mecklenburg L, Tobin DJ, Cirlan MV *et al.* (2005) Premature termination of hair follicle morphogenesis and accelerated hair follicle cycling in Iasi congenital atrichia (fzica) mice points to fuzzy as a key element of hair cycle control. *Exp Dermatol* 14:561–70

Moll R, Divo M, Langbein L (2008) The human keratins: biology and pathology. *Histochem Cell Biol* 129:705–33

Müller-Röver S, Handjiski B, van der Veen C *et al.* (2001) A comprehensive guide for the accurate classification of murine hair follicles in distinct hair cycle stages. *J Invest Dermatol* 117:3–15

Nowak JA, Fuchs E (2009) Isolation and culture of epithelial stem cells. *Methods Mol Biol* 482:215–32

Nowak JA, Polak L, Pasolli HA *et al.* (2008) Hair follicle stem cells are specified and function in early skin morphogenesis. *Cell Stem Cell* 3:33–43

Oda Y, Hu L, Bul V *et al.* (2012) Coactivator MED1 ablation in keratinocytes results in hair-cycling defects and epidermal alterations. *J Invest Dermatol* 132:1075–83

Peters JM, Lee SS, Li W *et al.* (2000) Growth, adipose, brain, and skin alterations resulting from targeted disruption of the mouse peroxisome proliferator-activated receptor beta(delta). *Mol Cell Biol* 20:5119–28

Plikus M, Wang WP, Liu J *et al.* (2004) Morpho-regulation of ectodermal organs: integument pathology and phenotypic variations in K14-Noggin engineered mice through modulation of bone morphogenic protein pathway. *Am J Pathol* 164:1099–114

Plikus MV, Mayer JA, de la Cruz D *et al.* (2008) Cyclic dermal BMP signalling regulates stem cell activation during hair regeneration. *Nature* 451: 340–4

Rhee H, Polak L, Fuchs E (2006) Lhx2 maintains stem cell character in hair follicles. *Science* 312:1946–9

Rittie L, Stoll SW, Kang S *et al.* (2009) Hedgehog signaling maintains hair follicle stem cell phenotype in young and aged human skin. *Aging Cell* 8:738–51

Sharov AA, Mardaryev AN, Sharova TY *et al.* (2009) Bone morphogenetic protein antagonist noggin promotes skin tumorigenesis via stimulation of the Wnt and Shh signaling pathways. *Am J Pathol* 175:1303–14

Stumpf M, Waskow C, Krotschel M *et al.* (2006) The mediator complex functions as a coactivator for GATA-1 in erythropoiesis via subunit Med1/TRAP220. *Proc Natl Acad Sci USA* 103:18504–9

Stumpf M, Yue X, Schmitz S *et al.* (2010) Specific erythroid-lineage defect in mice conditionally deficient for Mediator subunit Med1. *Proc Natl Acad Sci USA* 107:21541–6

Sundberg JP, Hogan ME (1994) Hair types and subtypes in the laboratory mouse. In: Sundberg JP (ed) *Handbook of Mouse Mutations with Skin and Hair Abnormalities*. CRC Press: Boca Raton, 57–68

Tarutani M, Itami S, Okabe M *et al.* (1997) Tissue-specific knockout of the mouse Pig-a gene reveals important roles for GPI-anchored proteins in skin development. *Proc Natl Acad Sci USA* 94:7400–5

Trempus CS, Morris RJ, Bortner CD *et al.* (2003) Enrichment for living murine keratinocytes from the hair follicle bulge with the cell surface marker CD34. *J Invest Dermatol* 120:501–11

Vidal VP, Chaboissier MC, Lutzkendorf S *et al.* (2005) Sox9 is essential for outer root sheath differentiation and the formation of the hair stem cell compartment. *Curr Biol* 15:1340–51

Wada O, Oishi H, Takada I *et al.* (2004) BRCA1 function mediates a TRAP/DRIP complex through direct interaction with TRAP220. *Oncogene* 23:6000–5

Zhou R, Bonneaud N, Yuan CX *et al.* (2002) SOX9 interacts with a component of the human thyroid hormone receptor-associated protein complex. *Nucleic Acids Res* 30:3245–52

Zhu Y, Qi C, Jain S *et al.* (1997) Isolation and characterization of PBP, a protein that interacts with peroxisome proliferator-activated receptor. *J Biol Chem* 272:25500–6

Zhu Y, Qi C, Jia Y *et al.* (2000) Deletion of PBP/PPARBP, the gene for nuclear receptor coactivator peroxisome proliferator-activated receptor-binding protein, results in embryonic lethality. *J Biol Chem* 275:14779–82